arXiv:1010.3704v1 [astro-ph.SR] 18 Oct 2010

The Supernova Impostor Impostor SN 1961V: *Spitzer* Shows That Zwicky Was Right (Again)

C. S. Kochanek[1,2], D. M. Szczygiel[1,2], K. Z. Stanek[1,2]

ABSTRACT

SN 1961V, one of Zwicky's defining Type V supernovae (SN), was a peculiar transient in NGC 1058 that has variously been categorized as either a true core collapse SN leaving a black hole (BH) or neutron star (NS) remnant, or an eruption of a luminous blue variable (LBV) star. The former case is suggested by its association with a decaying non-thermal radio source, while the latter is suggested by its peculiar transient light curve and its low initial expansion velocities. The crucial difference is that the star survives a transient eruption but not an SN. All stars identified as possible survivors are significantly fainter, $L_{opt} \sim 10^5 L_\odot$, than the $L_{opt} \simeq 3 \times 10^6 L_\odot$ progenitor star at optical wavelengths. While this can be explained by dust absorption in a shell of material ejected during the transient, the survivor must then be present as a $L_{IR} \simeq 3 \times 10^6 L_\odot$ mid-infrared source. *Using archival Spitzer observations of the region, we show that such a luminous mid-IR source is not present.* The brightest source of dust emission is only $L_{IR} \simeq 10^5 L_\odot$ and does not correspond to the previously identified candidates for the surviving star. The dust cannot be made sufficiently distant and cold to avoid detection unless the ejection energy, mass and velocity scales are those of a SN or greater. We conclude that SN 1961V was a peculiar, but real, supernova. Its peculiarities are probably due to enhanced mass loss just prior to the SN, followed by the interactions of the SN blast wave with this ejecta. This adds to the evidence that there is a population of SN progenitors that have major mass loss episodes shortly before core collapse. The progenitor is a low metallicity, $\sim 1/3$ solar, high mass, $M_{ZAMS} \gtrsim 80 M_\odot$, star, which means either that BH formation can be accompanied by an SN or that surprisingly high mass stars can form a NS. We also report on the mid-IR properties of the two other SN in NGC 1058, SN 1969L and SN 2007gr.

Subject headings: supernovae:general, supernovae: individual: SN 1961V, SN 1969L, SN 2007gr

1. Introduction

We know that stars both explode, as core-collapse SN, and erupt in luminous transients that eject mass but do not destroy the star. In some cases, both types of transients produce similar, Type IIn spectra, where the "n" indicates that the emission lines are narrow ($\lesssim$ 2000 km/s) compared to a normal supernova (Schlegel

[1]Department of Astronomy, The Ohio State University, 140 West 18th Avenue, Columbus OH 43210

[2]Center for Cosmology and AstroParticle Physics, The Ohio State University, 191 W. Woodruff Avenue, Columbus OH 43210

1990, Filippenko 1997). Type IIn SNe seem to be cases where the blast wave is interacting with a dense circumstellar medium created either by a massive wind or mass ejected in a pre-SN eruption (see, e.g., Smith et al. (2008), Gal-Yam et al. (2007) and references therein). The mechanism of the eruptions from LBV stars is not well-understood (see, e.g., Humphreys & Davidson 1994, Smith & Owocki 2006), but they eject material at velocities lower than normal SN. Unfortunately, the luminosities of the faintest SN are not well separated from those of the brightest eruptions, making it difficult to safely classify transients at the boundary. These brightest of stellar eruptions are frequently referred to as SN "impostors" (Van Dyk et al. 2002). Correct classifications are important for understanding the rates and mechanisms of both processes. In particular, we note the recent debates about the nature of SN 2008S and the 2008 transient in NGC 300 (see Prieto et al. (2010) and references therein).

The most obvious difference between the two cases is that the star survives only in the eruption scenario. Thus, there have been attempts to identify the surviving star for a number of the impostors, with candidates identified for SN 1954J (Smith et al. 2001, Van Dyk et al. 2005), SN 1961V (see below), SN 1997bs (Van Dyk et al. 1999, Li et al. 2002), and SN 2000ch (Wagner et al. 2004, Pastorello et al. 2010). It is probably safe to say that none of these identifications besides SN 2000ch is certain. There is, however, a second test. Most of the candidate survivors are fainter than the progenitors, and this is expected because the surviving star lies inside a shell of ejected material that probably forms dust as it cools. For the spectacular Galactic example of η Carina, $\sim$ 90% of the emission is absorbed and reradiated in the mid-IR (see Humphreys & Davidson (1994)). Thus, a good test for these identifications is to find the mid-IR emission from the survivor and check that it matches the absorption indicated by the difference between the luminosities of the progenitor and the survivor.[1] While some SN may be late time IR sources, they should evolve more rapidly and are unlikely to show the balance between progenitor luminosity, optical absorption and mid-IR emission expected for a surviving star. While frequently noted, this test never seems to have been carried out. We do so here for SN 1961V.

The progenitor of SN 1961V was (likely) the brightest star in NGC 1058, with $m_{pg} \simeq 18$ in the decades before the transient (Bertola 1964, Zwicky 1964). Utrobin (1987) estimated magnitudes in December 1954 of $B = 18.2 \pm 0.1$, $V = 17.7 \pm 0.3$, and $B-V = 0.6 \pm 0.3$. Given a distance of 9.3 Mpc, the Cepheid distance to fellow group member NGC 925 (Silbermann et al. 1996), and Galactic extinction of $E(B-V) = 0.06$ mag (Schlegel et al. 1998), this corresponds to $M_B \simeq -12$, making the progenitor one of the brightest stars in any galaxy. Detailed discussions of the light curve are presented in Doggett & Branch (1985), Goodrich et al. (1989), Humphreys & Davidson (1994), and Humphreys et al. (1999), based on the data obtained by Zwicky (1964), Bertola (1963), Bertola (1964), Bertola (1967), Bertola & Arp (1970), and Fesen (1985). Sometime between 1955 and 1960 the star started to brighten, reaching a plateau of $m_{pg} \simeq 14$ by the summer of 1961 before briefly peaking at $m_{pg} \simeq 12.5$ in December 1961. At this peak, it was brighter than the maximum of the Type IIP SN 1969L (e.g. Ciatti et al. 1971) and comparable to the peak of the Type Ic SN 2007gr (Valenti et al. 2008), the two other SN in NGC 1058. It then dropped in brightness, going through a series of extended plateaus, including a 4 year period from 1963 to 1967 where it was only moderately fainter than

[1]There can be problems in this accounting from binary companions (see Kochanek (2009)) and chance coincidences.

the progenitor, with $m_{pg} \simeq 19$. After 1968 it had faded below the point of visibility, $m_{pg} \gtrsim 22$. Spectra of the event were also peculiar (Branch & Greenstein 1971), with relatively narrow lines (FWHM $\simeq$ 2000 km/s), strong helium emission lines and a constant color, resembling an F star, near maximum light (Bertola 1965). Based on these peculiarities, Zwicky (1964) classified SN 1961V, along with η Carina, as a "Type V" supernova, although the clear presence of hydrogen in the spectra would lead to a "modern" classification of Type IIn or peculiar (Branch & Cowan 1985, Filippenko 1997).

Goodrich et al. (1989) proposed that the peculiar, extended light curve and low velocity spectra would be more easily explained if SN 1961V was actually an LBV eruption rather than an SN. They proposed that the progenitor was a hot ($T_* > 45000$ K), luminous ($L_* \simeq 10^{6.4} L_\odot$) star that was undergoing an S Doradus outburst in the decades prior to the eruption. During such an outburst, the star has the same bolometric luminosity but a far lower photospheric temperature ($T_* \simeq 8000$ K, see Humphreys & Davidson (1994)). This scenario requires a surviving star, and several candidates have been identified from a sequence of steadily improving Hubble Space Telescope images by Filippenko et al. (1995), Van Dyk et al. (2002) and Chu et al. (2004) based on the accurate optical (Klemola 1986) or radio (Branch & Cowan 1985, Cowan et al. 1988, Stockdale et al. 2001) positions. All proposed candidates are significantly fainter than the progenitor, with $V \simeq 24$ mag.

The primary counterargument to the LBV eruption hypothesis is that SN 1961V also seems to be associated with a fading, non-thermal radio source (Branch & Cowan 1985, Cowan et al. 1988, Stockdale et al. 2001, Chu et al. 2004) that closely resembles the properties of other radio SNe and not the fainter, thermal emission of η Carina. There is no non-thermal radio emission (or even a detection) from the SN impostor/LBV eruption SN 1954J even though it is almost four times closer and of similar age (Eck et al. 2002). VLBI observations in 1999 by Chu et al. (2004) also resolved out the radio emission, setting a minimum radius for the radio emission of order 4 mas or about 0.17 pc. This would require an expansion velocity of $v \gtrsim 4000$ km/s that would be hard to explain with an eruption.

While the Spitzer Space Telescope (SST) was not intended for studies of individual stars at 10 Mpc, it should have no difficulty identifying a source with the luminosity of the SN 1961V progenitor star in the outskirts of NGC 1058. Indeed, Goodrich et al. (1989) note that in the infrared the source should be "the brightest point thermal IR source in NGC 1058." Here we use archival SST IRAC (Fazio et al. 2004) and MIPS (Rieke et al. 2004) data to measure the infrared emission associated with SN 1961V. In §2 we discuss the available data, the astrometry relative to the HST data used to identify candidate surviving stars, and the resulting estimates and limits on the mid-IR luminosity. We model the photometry in §3 to find that there is insufficient infrared emission for the progenitor star to have survived and that SN 1961V must, therefore have been an SN. We note that Smith et al. (2010) have simultaneously reached this conclusion based on the gross differences between SN 1961V and other supernova impostor candidates and its greater similarity to other core-collapse SN. In §4 we present the photometry for SN 1969L and SN 2007gr, the other two SN in NGC 1058. In §5 we discuss the consequences of SN 1961V having been an SN.

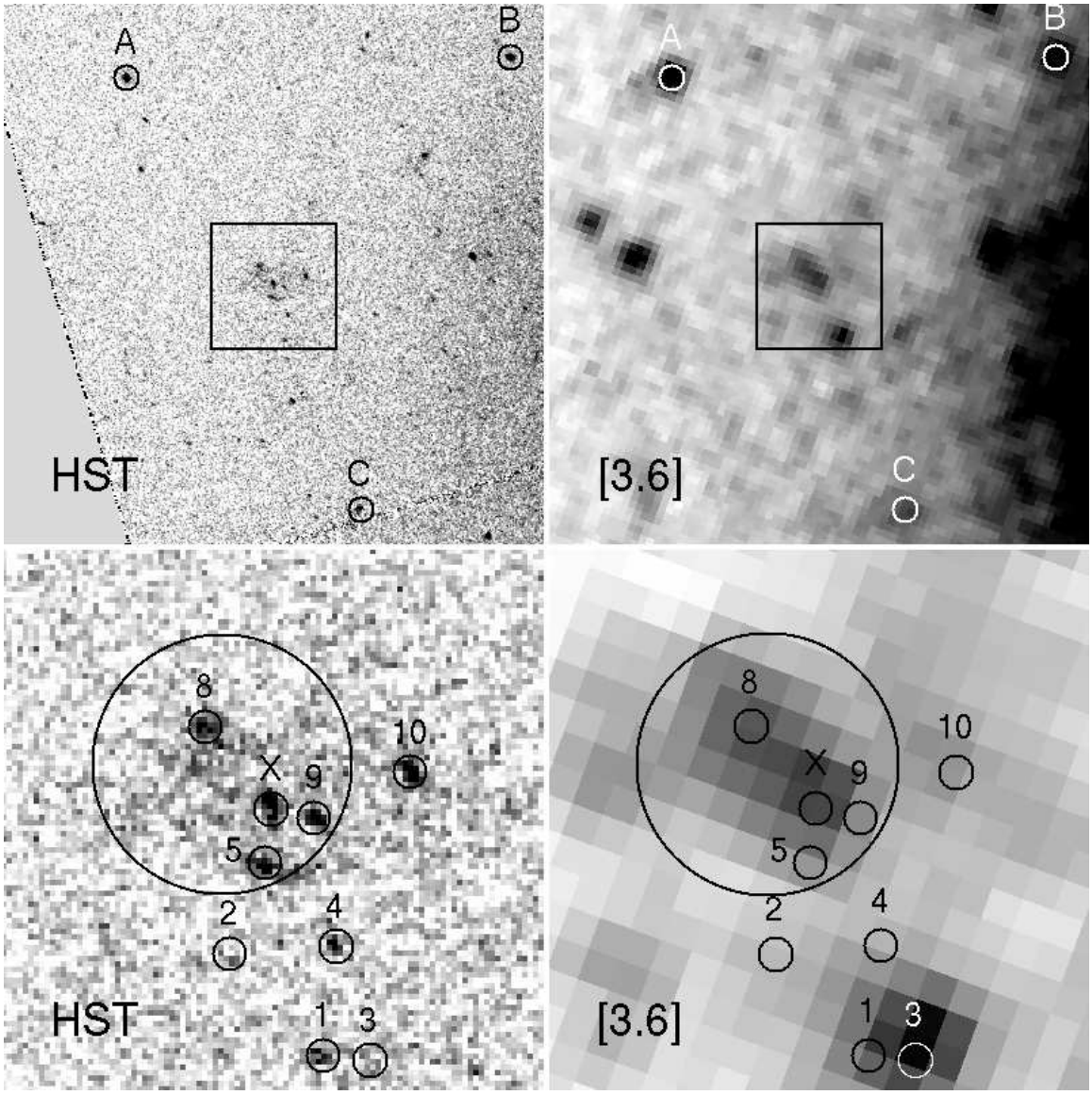

Fig. 1.— Astrometric matches between the F606W HST image and the 3.6μm reference image. The top panels show a 45″ field of view showing three stars (labeled A, B and C and marked by 1.″0 radius circles) that can be well-matched between the bands. The lower panels show a narrower 10.″0 region around SN 1961V corresponding to the box in the top panels, where we have labeled the sources following Van Dyk et al. (2002). The region labeled X marks the location of stars #6, 7, 9 and 11 from Van Dyk et al. (2002) and contains all the candidate surviving stars. Source #6 is brighter in the F814W image, and sources #3 and 11 are only detected in the F814W image. The small circles in the lower panels are 0.″3 in radius while the large circle corresponds to the 2.″4 radius photometry apertures shown in Fig. 2.

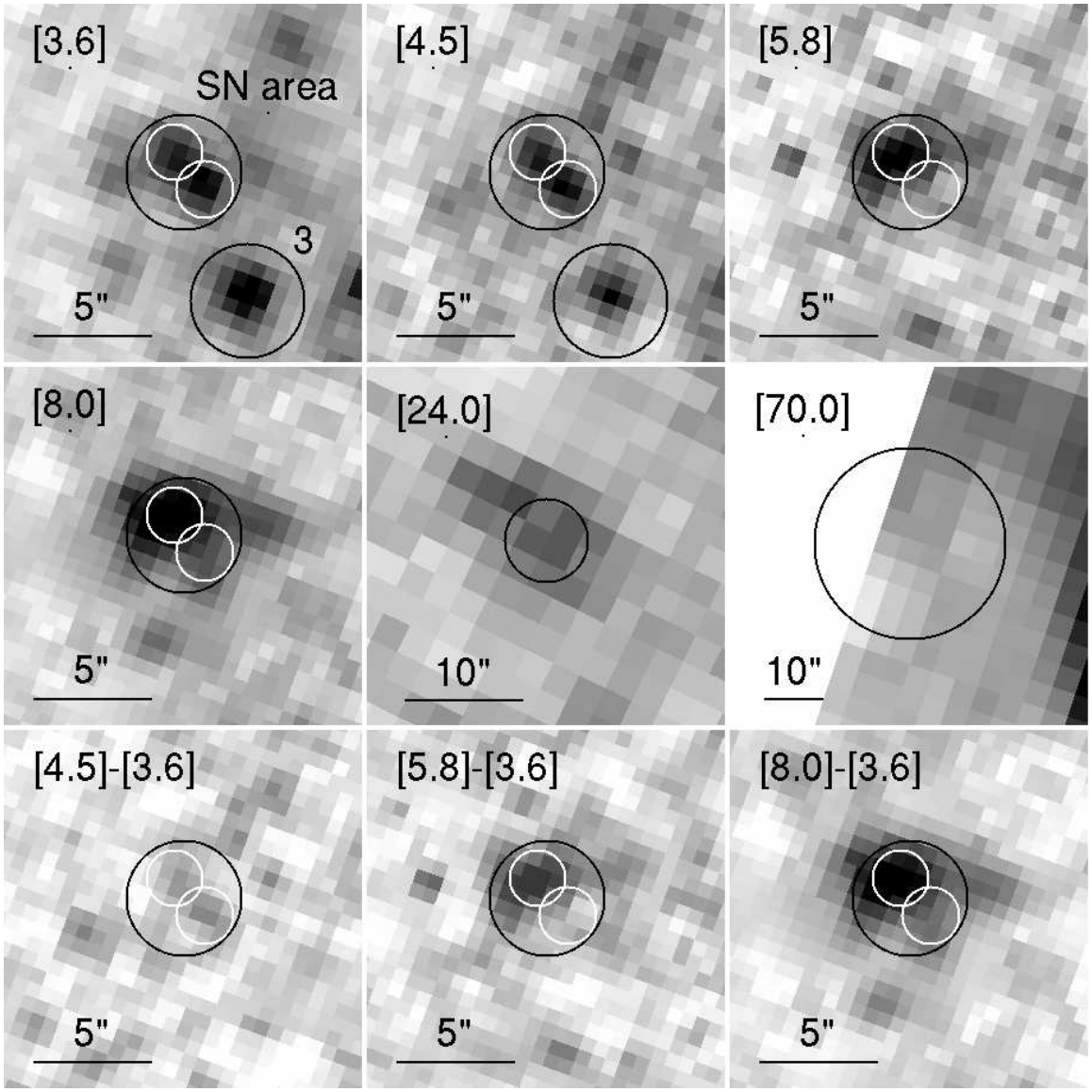

Fig. 2.— Mid-IR images and wavelength differenced images of the SN 1961V region. The top panels show the 3.6, 4.5 and 5.8μm images of the region, the middle panels show the 8.0, 24 and 70μm images of the region, and the lower panels show the [4.5] − [3.6], [5.8] − [3.6] and [8.0] − [3.6] wavelength differenced images. This removes the flux from normal stars to leave only sources of dust and PAH emission. The panels are 15.″0, 30.″0 and 60.″0 in size for the IRAC, 24μm and 70μm bands, respectively. The large black circles in the IRAC, 24 and 70μm panels have radii of 2.″4, 3.″4 and 16.″0, respectively, and correspond to the aperture sizes used for photometry. The smaller 1.″2 radius circles mark the positions of star #8 and the region X encompassing the candidate surviving stars. We also analyzed the IRAC images of the region using a 3.″6 radius aperture and DAOPHOT.

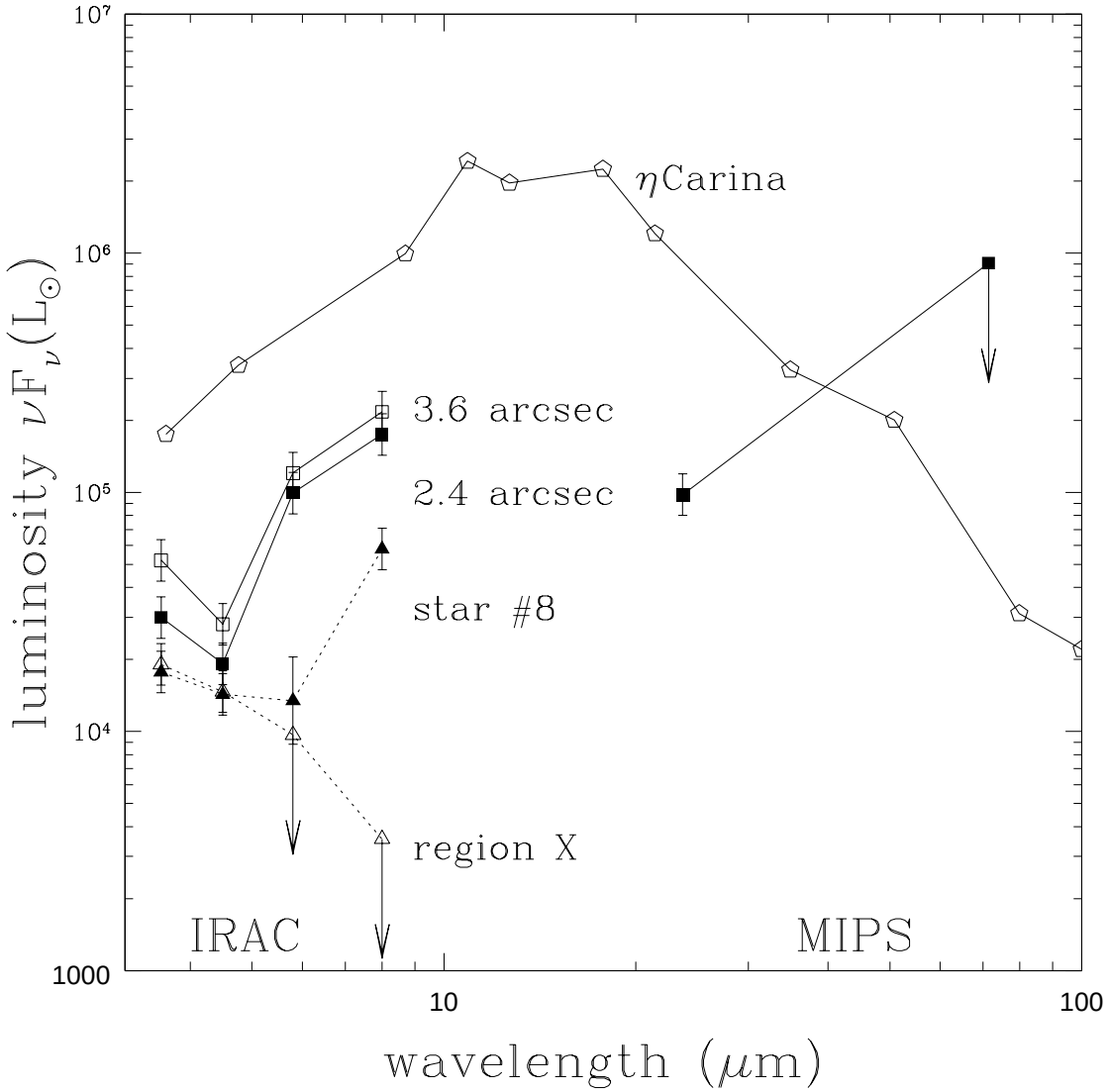

Fig. 3.— Mid-IR SEDs of the SN 1961V region. The total emission is described by the large aperture MIPS fluxes and either the 3.″6 (open squares) or 2.″4 (filled squares) IRAC apertures. With DAOPHOT we attempt to separate the fluxes of star #8 (filled triangles) and the region X (open triangles) that contains all the proposed surviving stars. For comparison, we show with open pentagons the SED of η Carina from Humphreys & Davidson (1994), which roughly has the properties we expect for SN 1961V. The 2.″4 IRAC apertures combined with the 24μm luminosity and the 70μm upper limit will be our standard comparison SED. Note that region X has an SED dropping to longer wavelengths, indicating it is dominated by stellar emission, while star #8 has an IR excess.

2. Data and Infrared Luminosity Estimates

NGC 1058 has been observed twice with IRAC and MIPS, as summarized in Table 1. The total exposure times are 15×30 s = 450 s for the IRAC bands, 10 s + 30 s = 40 s for the MIPS 24μm band and 3×3 s = 9 s for the MIPS 70μm band. The SST sensitivity estimates for these exposure times are 0.36, 0.62, 4.1, 4.7, 25 and 3400μ Jy, at 3.6, 4.5, 5.8, 8.0, 24 and 70μm, respectively. If we convert these into 3σ limits on νL_ν in each band at the distance to NGC 1058, they correspond to 2400, 3300, 17000, 14000, 25000 and $1.2 \times 10^6 L_\odot$ for the 3.6, 4.5, 5.8, 8.0, 24 and 70μm bands, respectively. In practice, we would be confusion limited in the IRAC bands were we trying to reach these detection limits, but, as Goodrich et al. (1989) noted, we should have little difficulty finding the expected $> 10^6 L_\odot$ mid-infrared source!

We downloaded the Post-Basic Calibrated Data (PBCD) for these programs from the Spitzer archive. These IRAC images are two-times oversampled and have a pixel scale of 0.″60, while the MIPS 24μm and 70μm images have pixel scales of 2.″45 and 4.″0 respectively compared to native pixel scales of 2.″55 and 5.″2 (narrow field of view). We aligned and combined the data for each band using the ISIS (Alard & Lupton 1998, Alard 2000) image subtraction package. We also used ISIS to difference image between the available epochs, to search for any signs of variability, and to difference image between wavelengths. The latter technique takes advantage of the fact that all "normal" stars have the "same" mid-IR colors, so normal stars effectively "vanish" to leave only the red stars dominated by dust emission and emission by the interstellar medium (see Khan et al. 2010). This wavelength differencing procedure isolates the relatively rare, dusty stars without the crowding from the normal stars. We also obtained the HST images used by Van Dyk et al. (2002) so that we could astrometrically match the Spitzer data with the progenitors discussed by Filippenko et al. (1995), Van Dyk et al. (2002) and Chu et al. (2004). We also examined the more recent images of the area from October 2007 (Van Dyk/11119) and August 2008 (Li/10877), but these do not significantly improve on the prior data.

Fig. 1 shows a wide field and close-up view of the SN 1961V region in the HST WFPC2 F606W (Illingworth/5446) and 3.6μm reference images. Clearly, with Spitzer's resolution we will be unable to obtain photometry for all the individual stars identified in the HST image, particularly at the longer wavelengths. We see counterparts in the 3.6μm image to star #8, the group of stars #5/6/7/9/11 (which we will refer to as region X) and star #3. Stars #3 and #11 are not visible in the F606W image, but are detected in the F814W image. The large black circle is 2.″4 in radius and represents one of the apertures we used for photometry.

Fig. 2 shows regions around SN 1961V for all 6 Spitzer bands. We used black circles to mark the 2.″4 photometric aperture we used to estimate the fluxes on IRAC images, as well as the 3.″5 and 16.″0 apertures used to measure fluxes in the 24.0 and 70.0μm MIPS bands respectively. For clarity, the alternative 3.″6 aperture used for the IRAC bands is not shown. We also show the wavelength differenced images between 3.6μm and the other three IRAC bands. We see that most of the sources in the 3.6μm image are normal stars, since they fade away at longer wavelengths and do not appear in the wavelength differenced images. There is some dust related emission, much of which seems to be associated with source #8, for which we lack an optical color because it lay just off the field edge in the F814W and F450W images analyzed by

Van Dyk et al. (2002), and possibly with source #10. Chu et al. (2004) identify star #7 as the only point-like source of Hα emission. The complex of sources corresponding to stars #6, 7, 9 and 11 in Van Dyk et al. (2002), which we have labeled region X in Fig. 1, appears to have no significant excess emission due to dust even though they correspond to all the claimed counterparts to SN 1961V (see below).

We estimated the fluxes using two procedures. First, we simply used aperture photometry (the IRAF apphot package). We used signal aperture radii (background annuli) of 2.″4 (2.″4-7.″2) and 3.″6 (3.″6-8.″3) for the IRAC bands, 3.″5 (6.″0-8.″0) at 24μm and 16.″0 (18.″0-39.″0) at 70μm. The background was estimated using the mode of the background pixels after 2σ outlier rejection, an approach which should work reasonably well in crowded regions. We also compensated for the presence of the edge of the 70μm image. No source was identified at 70μm, so we estimated a 3σ upper limit on the flux. We used the standard Spitzer corrections for these apertures.[2] For the 2.″4 (3.″6) IRAC aperture these are 1.213, 1.234, 1.379 and 1.584 (1.124, 1.127, 1.143 and 1.234) for the 3.6μm, 4.5μm, 5.8μm and 8.0μm bands, respectively, with uncertainties of order 1–2%. For the 24 and 70μm apertures, they are 2.80 and 2.07 and are accurate to about 5%. The resulting flux estimates are presented in Tables 2 and 3.

While the large aperture photometry provides a conservative upper limit on the luminosity of any individual source, it is clear that the flux near SN 1961V can be divided over several sources in the IRAC images. To better account for the effects of overlapping PSFs than is possible with aperture photometry, we also analyzed the region with DAOPHOT (Stetson 1987), in particular dividing the IRAC flux between source #8 and the complex of sources in region X associated with the candidate surviving stars. For the still lower resolution MIPS images, no attempt was made to divide the flux over sub-components. The DAOPHOT results are also presented in Table 2. Fig. 3 compares these estimates to each other as well as to the SED of η Carina from Humphreys & Davidson (1994). The total flux, even in the large apertures, is far less than that of η Carina, which roughly has the luminosity and SED we expect for SN 1961V. The sub-components are then significantly less luminous, although the DAOPHOT division into two sources does not capture all the flux in the aperture, and we again see that while star #8 has an IR excess, the region X containing all the proposed surviving stars seems not to. We also checked for variability in the IRAC and 24μm bands, finding none to limits of roughly 10%.

We also report photometry for Stars A, B and C in Fig. 1, Van Dyk et al. (2002) star #3, SN 1969L (Ciatti et al. 1971) and SN 2007gr (Crockett et al. 2008, Valenti et al. 2008). The location of SN 1969L was only covered by some of the images and SN 2007gr is only present in the later data, so we only analyzed the relevant images but followed the same procedures. We only obtained upper limits on any flux from SN 1969L, while SN 2007gr was a very bright source. We discuss the results for these SN in §4.

[2]http://ssc.spitzer.caltech.edu/irac/iracinstrumenthandbook/ and http://ssc.spitzer.caltech.edu/mips/mipsinstrumenthandbook/

3. Models

We model the spectral energy distributions (SED) using DUSTY (Ivezić & Elitzur 1997, Ivezić et al. 1999, Elitzur & Ivezić 2001). We assumed a dusty shell with a density distribution $\propto 1/r^2$ and an outer radius at twice the distance of the inner, $R_{out} = 2R_{in}$. This assumption has little affect on the results. The models are specified by the temperature of the illuminating black body, the stellar temperature T_*, the optical depth of the shell τ_V at V band, and the dust temperature T_d at the inner edge of the shell. We tabulated the models for Draine & Lee (1984) graphitic and silicate dusts with the standard size distributions assumed by DUSTY for stellar temperatures of T_* = 5000, 7500, 10000, 15000, 20000, 30000 and 40000 K, inner edge dust temperatures from 50 to 900 K in steps of 50 K, and V-band optical depths of τ_V = 0 to 6 in steps of 0.1 and τ_V = 6 to 30 in steps of 0.5. Our approach will be to normalize the models based on the pre-transient luminosity and then constrain the optical depth to match the flux of the candidate survivors, leaving as the remaining variable the dust temperature.

Given the stellar luminosity, the dust temperature is determined by the shell radius, and the shell radius is closely related to the physics of the transient. Since the progenitor must have been essentially unobscured pre-transient[3], we know that any obscuring material must have been ejected in 1961. If the velocity is restricted by the FWHM of the optical lines, roughly 2000 km/s (e.g. Branch & Greenstein 1971), then the current radius of the material is

$$R \simeq 1.4 \times 10^{17} \left(\frac{v_{ej}}{1000 \text{ km/s}} \right) \text{ cm} \tag{1}$$

where we set the elapsed time to 43 years (1961 to 2004) and the velocity v_{ej} to half of the FWHM. In our standard models we consider those with inner shell radii near this value, which is mildly conservative given that the inner edge dominates the dust emission. The outer edge is then at twice this distance and so has twice the expansion velocity.

The only way to escape our eventual limits is to make the dust so cold that it cannot be detected given Spitzer's diminishing sensitivity at longer wavelengths. For the dust temperature to be low, the dust must be distant, and for the simple case of radiative equilibrium for dust radiating as a black body, the dust temperature is

$$T = \left(\frac{L_*}{16\pi\sigma R^2} \right)^{1/4} = 142 \left(\frac{L_*}{3 \times 10^6 L_\odot} \right)^{1/4} \left(\frac{10^{17} \text{ cm}}{R} \right)^{1/2} \text{ K} \tag{2}$$

(e.g. Wright (1980)) corresponding to an SED peaking near $\lambda = 20\mu$m that will be strongly constrained by the 24μm data. DUSTY, with better dust emissivity models, usually predicts higher inner edge dust temperatures than this simple model but a similar peak emission wavelength. Lowering the dust temperature to raise the peak wavelength requires a larger dust radius, but moving the shell to a larger radius requires

[3]Otherwise, its already high luminosity would quickly exceed $10^7 L_\odot$ after extinction corrections! Adding additional unrelated foreground extinction only strengthens our conclusions because it will adjust the progenitor luminosity upwards without contributing to the mid-IR flux.

rapid increases in both the ejected mass and energy. The V-band optical depth of the shell is

$$\tau_V = \frac{M_{ej}\kappa_{opt}}{4\pi R_{in}R_{out}} \simeq 8\left(\frac{M_{ej}}{M_\odot}\right)\left(\frac{\kappa_{opt}}{500\ \mathrm{cm}^2/\mathrm{g}}\right)\left(\frac{R_{out}}{R_{in}}\right)\left(\frac{10^{17}\mathrm{cm}}{R_{in}}\right)^2 \tag{3}$$

where $\kappa_{opt} \simeq \kappa_{500} = 500\ \mathrm{cm}^2/\mathrm{g}$ is the optical opacity for a dust to gas ratio of roughly 1% (e.g. Semenov et al. 2003), M_{ej} is the ejected mass in which the dust forms, and the shell has a density profile $\propto 1/r^2$ from $R_{in} < R < R_{out}$. Equivalently, the required mass is

$$M_{ej} = 0.13\tau_V\left(\frac{\kappa_{500}}{\kappa_{opt}}\right)\left(\frac{R_{in}}{R_{out}}\right)\left(\frac{R_{in}}{10^{17}\mathrm{cm}}\right)^2 M_\odot. \tag{4}$$

Assuming a thin shell with $R_{in} \simeq R_{out} = R$ for simplicity, the energy of the ejecta,

$$E_{ej} = \frac{1}{2}M_{ej}v_{ej}^2 = 7\times 10^{47}\tau_V\left(\frac{\kappa_{500}}{\kappa_{opt}}\right)\left(\frac{R}{10^{17}\mathrm{cm}}\right)^4\ \mathrm{ergs}, \tag{5}$$

increases very rapidly with increasing shell radius because both the velocity and mass must be larger for larger distances. The energy required reaches an SN-like magnitude of 10^{51} ergs for $R \simeq 6\times 10^{17}\tau_V^{-1/4}$ cm, as does the velocity and mass. Making the dust distant enough to be cold forces the mass, velocity and energy budgets out of the LBV transient range. Phrasing the scaling in terms of the peak wavelength, $M_{ej} \propto \lambda_{peak}^4$ and $E_{ej} \propto \lambda_{peak}^8$, further emphasizes the problem with this solution. Using a thick shell exacerbates these problems since it leads to a larger mass-weighted radius.

In order to understand the mid-infrared limits we must first choose which HST star to call the survivor (see Fig. 1). Filippenko et al. (1995) propose star #6, with B and V magnitudes of 24.82 ± 0.25 and 24.50 ± 0.16 mag. Van Dyk et al. (2002) propose star #11, which they estimate to have an I magnitude of 24.3 ± 0.22, $B-I > 1$ and $V-I > 1.1$ mag. Chu et al. (2004) propose star #7 from Van Dyk et al. (2002), with B, V and I magnitudes of 24.04 ± 0.14, 23.85 ± 0.14 and 23.83 ± 0.14, respectively. Chu et al. (2004) prefer this identification because (1) it appears to be spatially coincident with the radio source, (2) it appears to be the only Hα source, and (3) its Hα line has broad wings (at least $\pm$550 km/s, limited by the noise in the spectrum). It does not, however, have the forbidden lines ([OI] λ6300Å, [OIII] λ4959/5007Å) expected from a remnant, suggesting the Hα emission is stellar. It is also too blue to be well-modeled as an extincted (hot) star, as noted by Chu et al. (2004). Of the Van Dyk et al. (2002) candidates closest to the preferred positions, #5 and #9 also have the wrong spectral slopes, while #6 and #11 are easily fit. Star #8, which has not been proposed as a candidate because it is too distant, is the only nearby source with significant dust emission (see Figs. 2 and 3).

In practice, it matters little which star we use for the survivor. They are all faint compared to the progenitor star and so must be heavily extincted in the optical. Once most of the optical/UV flux must be absorbed, it matters little for the expected mid-IR luminosities whether it is 90% or 99%. Similarly, the spectral shape of the candidate matters little, since the optical depth is principally determined by the magnitude difference between the survivor and the progenitor rather than the color. Thus, for simplicity we will simply give the survivor the typical magnitude of the candidates, $V = 24$ mag, and ignore the colors.

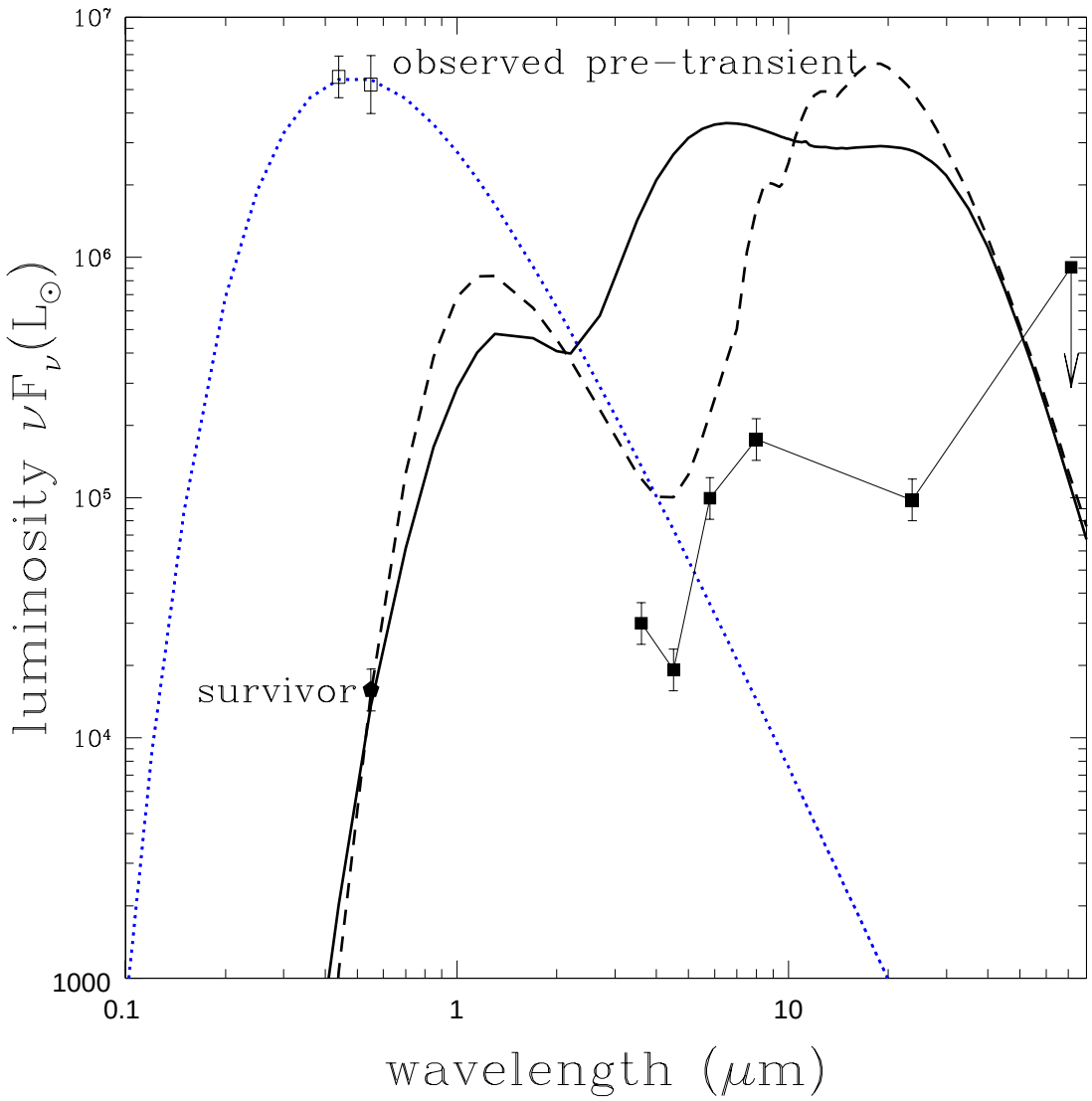

Fig. 4.— Models normalized by the pre-outburst magnitudes of Utrobin (1987). The predicted SEDs for graphitic (silicate) dust shown by the heavy solid (dashed) curves lie far above the *total* mid-IR emission (filled squares) from the SN 1961V region let alone that of any sub-component (see Fig. 3). In this case, the progenitor model (light solid curve) is a $T_* = 7500$ K black body normalized to match the pre-outburst magnitudes (open squares) from Utrobin (1987). The progenitor luminosity is $L_* = 10^{6.9} L_\odot$ and it would increase, leading to larger discrepancies, if we used a higher or lower stellar temperature. The V band optical depths are chosen to match the luminosity corresponding to our generic $V = 24$ mag extincted, surviving star (filled pentagon), and the inner shell radius is set to be close to 10^{17} cm.

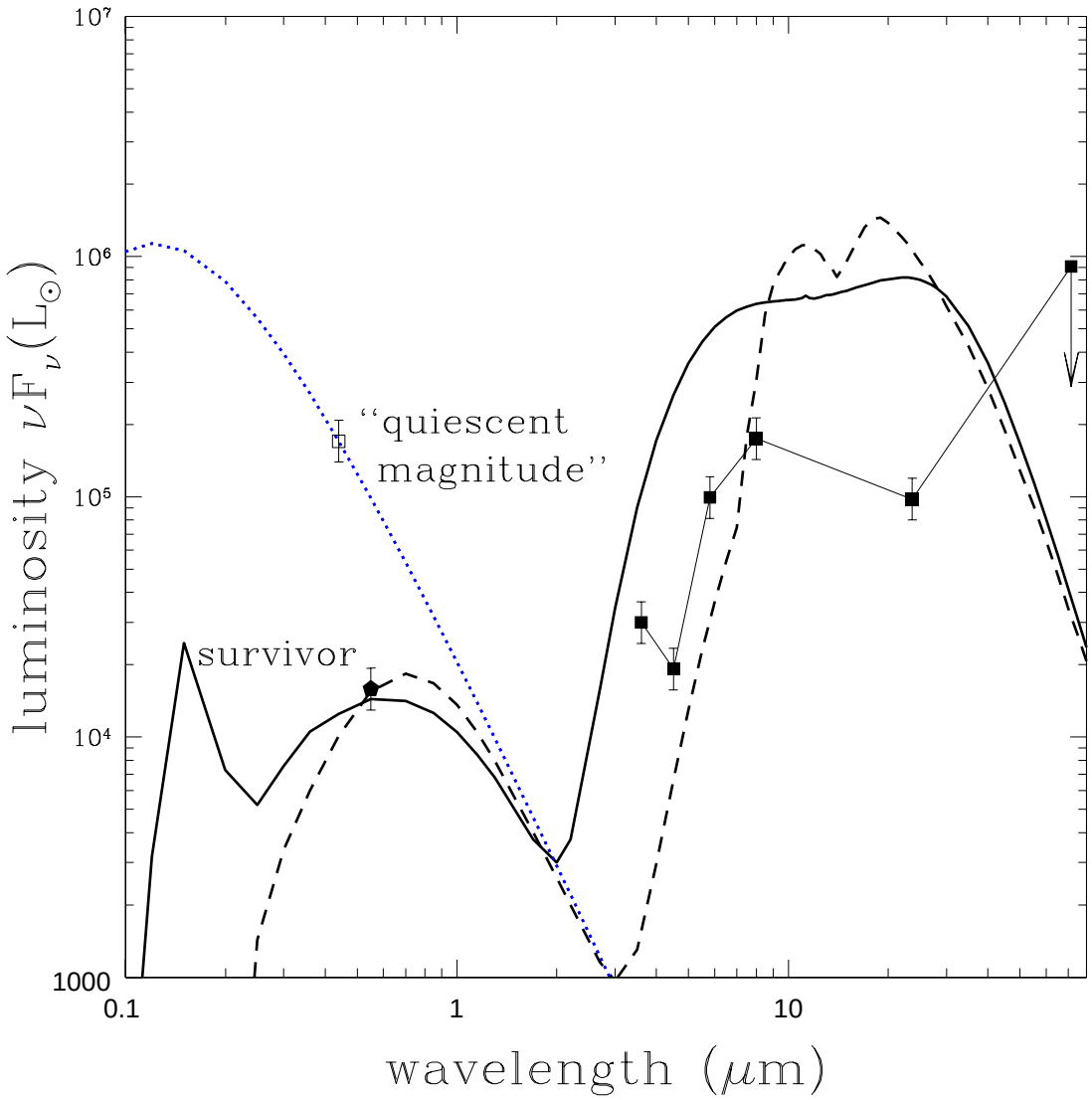

Fig. 5.— Models following the Goodrich et al. (1989) scenario. The predicted SEDs for graphitic (silicate) dust shown by the heavy solid (dashed) curves still lie well above the *total* mid-IR emission (filled squares) from the SN 1961V region let alone that of any sub-component (see Fig. 3). In this case, the progenitor model (light solid curve) is a $T_* = 30000$ K black body normalized to match the Goodrich et al. (1989) normalizing magnitude of $B = 22$ mag, leading to a stellar luminosity of $L_* = 10^{6.2} L_\odot$ that is somewhat low. The V band optical depths are again chosen to match the luminosity corresponding to our generic $V = 24$ mag extincted, surviving star (filled pentagon), and the inner shell radius is set to be close to 10^{17} cm. For $T_* = 40000$ K, L_* would double and be closer to matching the luminosity in Fig. 4, which would also double the mid-IR discrepancy.

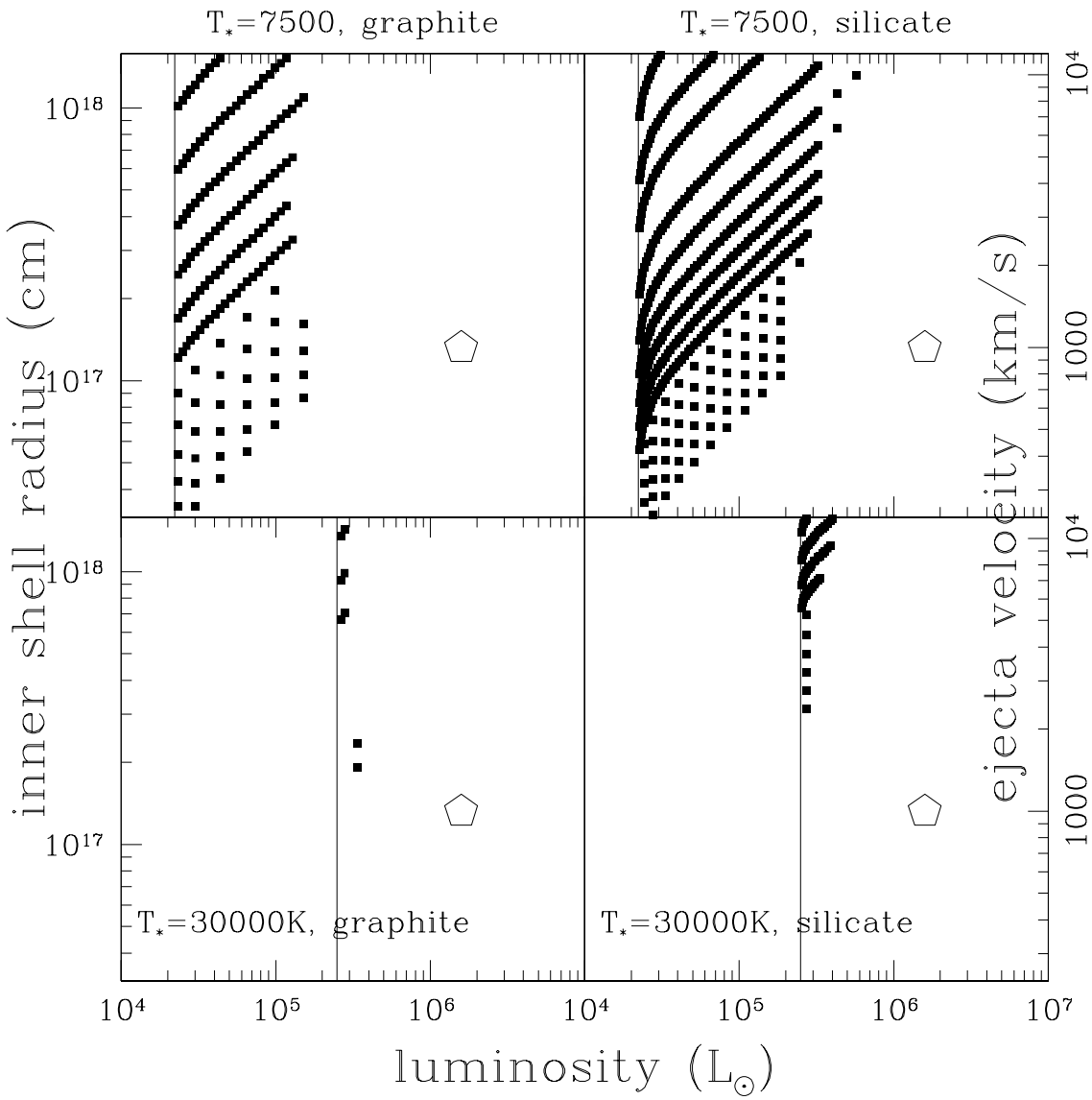

Fig. 6.— Stellar luminosities and shell radii (left scale) or ejecta velocities (right scale) that fit both the generic V = 24 mag extincted luminosity of the candidate survivors and roughly stay below the upper bound on the mid-IR emission ($\chi^2 < 24$ in Eqn. 6) for cold (T_* = 7500 K, top) and hot (T_* = 30000 K, bottom) stars and either graphitic (left) or silicate (right) dust. The vertical lines indicate the minimum (τ_V = 0) luminosity consistent with a V = 24 mag survivor. The open pentagon marks the solution with the properties typically associated with LBV transient hypothesis at $L_* = 10^{6.2} L_\odot$ and v_{ej} = 1000 km/s.

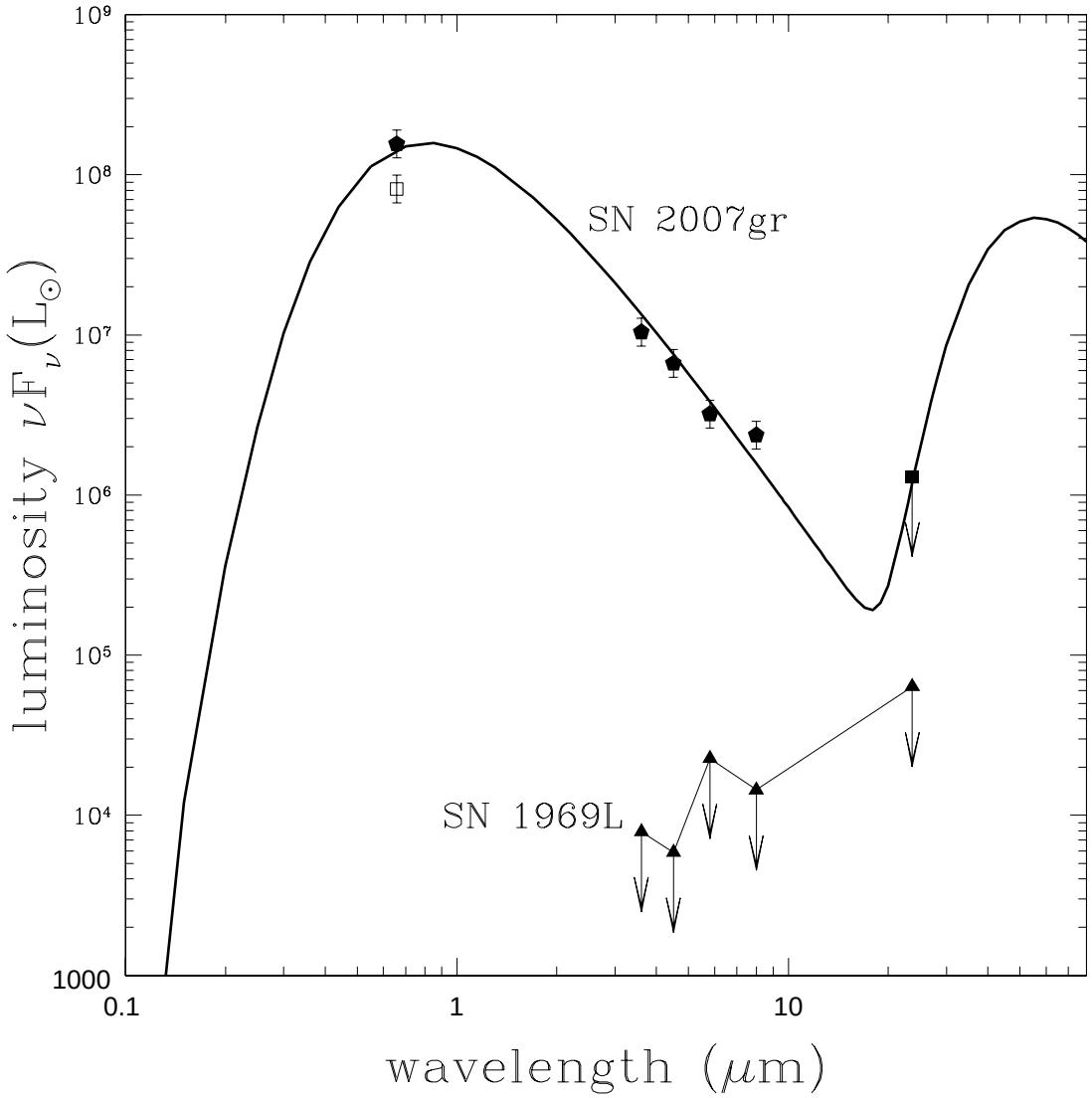

Fig. 7.— Limits on the mid-IR SED of SN 1969L (filled triangles) and the observed SED of SN 2007gr (filled squares). The filled R-band point from Valenti et al. (2008) corresponds to the epoch (+17 days) of the IRAC observations while the open point corresponds to the epoch (+31 days) of the MIPS observations. The heavy solid curve is a 5000 K black body with luminosity $10^{8.4} L_\odot$.

We have two possible choices for the intrinsic properties of the star. First, we can simply normalize it using the pre-transient luminosities. Alternatively, we can follow Goodrich et al. (1989) and assume that the star was in an S Doradus phase just before the transient and has now returned to its hotter, but similar luminosity quiescent state. If we set the stellar temperature to $T_* = 7500$ K and normalize it by the Utrobin (1987) magnitudes, we get a luminosity of $L_* \simeq 10^{6.9} L_\odot$. This is higher than the Goodrich et al. (1989) proposal of $10^{6.4} L_\odot$, but matches their proposed S Doradus outburst temperature and agrees tolerably well with the $B-V$ color from Utrobin (1987). Both raising and lowering the assumed temperature increases the luminosity because for $T_* = 7500$ K the peak of the SED lies near the normalizing photometric bands. In fact, with any significant change in the temperature, the luminosity becomes impossibly large ($L_* > 10^7 L_\odot$).

Fig. 4 shows the resulting models. Dust optical depths of $\tau_V = 7$ and 11.5 for graphitic and silicate dusts lead to enough extinction to make the optical flux consistent with a $V = 24$ mag flux for the surviving star. Choosing inner edge dust temperatures of $T_d = 500$ and 300 K corresponds to putting the inner edge for the dusty shell at $R \simeq 1.3 \times 10^{17}$ cm. The outer edge dust temperatures are roughly 140 K. Using a thin shell, with $R_{out} = 1.2 R_{in}$ instead of $2R_{in}$ leads to no significant changes. It is immediately apparent that the predicted mid-IR emission is grossly discrepant with the constraints even when we compare the model to the integrated emission from the region (defined here by the $2\farcs4$ IRAC fluxes and the MIPS aperture fluxes) without any division of the emission over the multiple sources within it (see Fig.3). The cool stellar temperature exacerbates the problem because much of the near-IR emission is little affected by extinction.

The alternate hypothesis, that the star has reverted to a quiescent hot state (Goodrich et al. 1989), changes things little. Here we assume that the surviving star has now left its S Doradus phase, and again has a high photospheric temperature with a quiescent magnitude that is 4 mag fainter than before the eruption, $B \simeq 22$ mag. For black bodies with $T_* = 30000$ K and 40000 K, this implies luminosities of $L_* = 10^{6.2} L_\odot$ and $L_* = 10^{6.5} L_\odot$ that are significantly below that implied by the pre-eruption luminosities, as also noted by Humphreys et al. (1999). Fig. 5 presents the $T_* = 30000$ K models. The visual optical depths are now much smaller ($\tau_V = 2.5$ and 4.5 for graphitic and silicate dusts) because most of the flux is in the UV where the dust opacities are higher. Choosing inner edge dust temperatures of $T_d = 400$ and 300 K corresponds to putting the inner edge for the dusty shell at roughly $R \simeq 1.5 \times 10^{17}$ cm. The outer edge dust temperatures are roughly 100 K. Again, using a thin shell leads to no significant changes. The discrepancies are smaller here, partly because the stellar luminosity is a factor of 5 lower than in the models of Fig. 4, and partly because the star has little near-IR luminosity compared to the cooler model. Nonetheless, the predicted mid-IR fluxes are still much higher than allowed by the observations. Raising the stellar temperature to $T_* = 40000$ K in order to better match the pre-transient luminosity or the Goodrich et al. (1989) models makes the problem worse by a factor of two.

In the end, the two most important variables are the intrinsic luminosity and the radius of the dust shell, or equivalently the ejection velocity of the material. We can explore these models by normalizing our DUSTY models to fit the generic $V = 24$ mag of the obscured progenitor star and then keeping only the models consistent with the total luminosity of the region, $L_{obs}(\lambda_i)$, again defined by the $2\farcs4$ aperture IRAC luminosities and the MIPS aperture luminosities and limits. The shell radius, or equivalently the expansion velocity, is the primary secondary variable. We can quantify the consistency using the mid-IR luminosities

for the region as luminosity limits based on the metric

$$\chi^2 = \sum_i \left(L_{mod}(\lambda_i)/L_{obs}(\lambda_i)\right)^2 \tag{6}$$

where λ_i corresponds to the 6 Spitzer bands, $L_{obs}(\lambda_i)$ is the Spitzer luminosity limit and $L_{mod}(\lambda_i)$ is the luminosity predicted by the model. An SED passing exactly through these 6 values or limits would have $\chi^2 = 6$, while those that are too bright will have higher values and those that are fainter will have lower values. At least for the IRAC bands, we know that these large aperture luminosities are subdivided over multiple sources and so are upper limits even if any of the source identifications are correct. In Fig. 6 we show all cases with $\chi^2 < 24$, which corresponds to the typical model luminosity being twice the observed upper limit, for stellar temperatures of $T_* = 7500$ and 30000 K and for graphitic and silicate dusts. As the secondary parameter we use the radius of the inner edge of the shell, or equivalently the expansion velocity of the shell. We only show cases with $\tau_V \geq 0.1$.

If the star is hot, $T_* = 30000$ K, then the stellar luminosity has to be at least $L_* > 10^{5.2} L_\odot$ in order to fit the optical luminosity of the surviving star. This is already high enough to make it very difficult to fall below the upper limits on the mid-IR luminosities in the presence of any dust. A few silicate models work by putting the shell so far out that the dust is cold enough to avoid all but the weak 70μm limit or by making the optical depth significantly less than unity. More solutions are possible when the star is $T_* = 7500$ K, because the star is intrinsically less luminous for the same V band normalization. We see the expected trend allowing more luminous stars for more distant and colder shells. There are no solutions in the regime required by the LBV eruption hypothesis.

We see no signs of variability in the mid-IR at the level of about 10% of the IRAC fluxes, although we would not expect to given the limited time baseline. While the existing data is not of high enough quality to make the test, we note that the optical variability should be significant given the parameters of our models. As the optical depth drops, the source should become steadily brighter, as is observed for η Carina (e.g. Humphreys & Davidson 1994, Humphreys et al. 1999). If we normalize the optical depth to τ_1 and time t_1, the optical depth scales as $\tau = \tau_1(t_1/t)^2$ (Eqn. 3), although the expected magnitude does not simply scale with τ because it includes both scattering and absorption. If we take $\tau_V = 4.5$ from the silicate models for a hot star, then a $V = 24.0$ mag progenitor in 2004, then it should have been 25.7 mag in 1995, and should be 23.4 mag in 2010, 23.1 mag in 2015, and 22.9 mag in 2020. In the cool star models the evolution is even more dramatic because of the higher optical depths. As Chu et al. (2004) noted, there is no sign of optical variability in the published data.

4. SN 1969L and SN 2007gr

Since we were analyzing the Spitzer data already, we measured the fluxes associated with the other two SN in NGC 1058, SN 1969L and SN 2007gr, reporting their fluxes in Tables 2 and 3 and presenting their SEDs in Fig 7. SN 1969L lay outside the 70μm image, and the image was taken before SN 2007gr, so we have no information on their 70μm fluxes. We detected no flux above background at the location

of SN 1969L (Ciatti et al. 1971), at limits on νL_ν of 10^4 to $10^5 L_\odot$. Here we used the 3σ upper bounds from the $3\farcs6$ radius IRAC aperture and the normal 24μm aperture. The observations of Type Ic SN 2007gr (Crockett et al. 2008, Valenti et al. 2008) were taken 17 (IRAC) and 31 (MIPS) days after the R-band peak. The mid-IR luminosities are comparable to what was expected for SN 1961V, with luminosities νL_ν of $10^{7.0}$, $10^{6.8}$, $10^{6.5}$, $10^{6.4}$ and $10^{6.1}$ for the 3.6, 4.5, 5.8, 8.0 and 24μm bands respectively. The SED, as shown in Fig. 7, is falling rapidly in the mid-IR, indicating that the emission is not dominated by a cool dust echo. We estimated R-band magnitudes at the two epochs of 13.6 and 14.3 mag based on the light curve in Valenti et al. (2008). The combined optical and mid-IR SED is well fit as a 5000 K black body with a luminosity of $10^{8.4} L_\odot$. If we look at the wavelength differenced 4.5μm image from before the SN, there does appear to be excess emission, consistent with the presence of the stars having K band excesses in Crockett et al. (2008), but with the resolution of Spitzer and the presence of bright stars just North and South of the site, we cannot say more.

5. Discussion

The basic conundrum is simple. All possible surviving stars are far fainter than the progenitor in the optical. This requires significant visual optical depths so that most of the surviving star's luminosity is re-radiated in the mid-IR. However, this opacity must be supplied by the material ejected during the transient, and dusty shells ejected at the low velocities of the LBV hypothesis and irradiated by a surviving star lead to mid-IR luminosities in gross conflict with the observational limits. The discrepancy is not a subtle problem, but a disagreement of an order of magnitude or more. The limits could be evaded by pushing the shell so far outward in radius that the dust temperature is too low to have significant emission in the 3.6 to 24μm range, but this solution requires shell masses, velocities and energies that are extreme even for a true SN. The simplest solution to these problems is that SN 1961V was in fact a supernova and there is no surviving star.

To escape the conclusion that SN 1961V was a supernova requires that an assumption about the properties of the star or its surrounding dust is greatly in error. We can enumerate three possibilities for changes in the stellar properties: (1) the system was (bolometrically) super-luminous for ~ 3 decades prior to the transient; (2) the surviving star has been (bolometrically) sub-luminous for the ~ 5 decades after the transient; and (3) there is no dust and the star now has a very high photospheric temperature, $T_* \simeq 70000$ to 100000 K, so that the faintness of the survivor is entirely due to bolometric corrections. In (1) and (2), the change in bolometric luminosity must be an order of magnitude or more. In case (3), such a radical increase in photospheric temperature would have be accompanied by significant mass loss which would be hard to reconcile with the requirement for no dust. Deeper ultraviolet observations than the available GALEX data would constrain this possibility, The remaining possibility is that the dust covering fraction is very small, less than 10%, with our line of sight coincidentally passing through one of the optically thick patches. The mid-IR emission is then reduced by the covering fraction. In this scenario we should still see the steady optical brightening created by an expanding shell. None of these possibilities seems terribly attractive or plausible.

If SN 1961V was a supernova, then it becomes one of the rare SNe with observations of its progenitor star, and the only one with a relatively detailed pre-explosion light curve (see Smartt 2009). We know it was very luminous, $L_* \sim 10^{6.3} L_\odot$, and likely hot in quiescence following the arguments of Goodrich et al. (1989). Based on the emission line ratios reported by Goodrich et al. (1989) for the Western HII region (the Eastern HII region overlaps the region with SN 1961V and shows evidence for contamination by a SN remnant), we estimate an oxygen abundance of approximately 8.3 following Kewley & Ellison (2008) or approximately $\sim 1/3$ Solar and similar to the metallicity of the LMC. This local measurement is a little lower than estimates of $\sim 1/2$ Solar from the metallicity gradient measurements by Ferguson et al. (1998). If we select stars at the end points of the Padua (Marigo et al. 2008) isochrones with $10^{6.1} L_\odot < L_* < 10^{6.5}$ and 20000 K $< T_* <$ 40000 K, they correspond to very massive stars, with $M_{ZAMS} > 80 M_\odot$ for all metallicities from LMC to Solar.

These properties are very similar to those of the only other high mass progenitor to be identified, that of SN 2005gl (Gal-Yam et al. 2007, Gal-Yam & Leonard 2009). For their measurements and parameters (a progenitor with $V = 20.04 \pm 0.15$ mag at 66 Mpc with $E(B-V) \simeq 0.07$), this progenitor had a luminosity similar to that of SN 1961V, with $L_* \simeq 10^{6.7} L_\odot$ for $T_* = 20000$ K. Like SN 1961V it was a Type IIn, and it had a comparable peak luminosity, near $M_V \sim -17$ mag. Gal-Yam et al. (2007) and Gal-Yam & Leonard (2009) propose that the spectral properties of SN 2005gl are best explained by heavy mass loss or mass ejections closely correlated with the SN. In fact, there is growing evidence that pre-supernova bursts of mass loss, while not common, are also not rare. The most remarkable case is the eruption observed two years prior to the peculiar Type Ib SN 2006jc (Pastorello et al. 2007), but the light curves of other SN show strong evidence for mass ejection episodes shortly before the SN (e.g., SN 2006gy, SN 2005ap, SN 2006tf, SN 2007va, see, e.g., Smith et al. (2008), Kozlowski et al. (2010)). The case of SN 2006jc may be particularly apt since the spectral evidence for excess helium (Branch & Greenstein 1971) suggests that SN 1961V was close to being a Type Ib rather than a Type IIn/pec.

Suppose we interpret SN 1961V in this context. In this view, the pre-SN light curve of SN 1961V is mapped into the pre-SN history of mass loss, and these phases of mass loss are then mapped into the post-SN light curve. We modify the Goodrich et al. (1989) scenario as follows. In quiescence, the progenitor is a hot star with a low density fast wind. Sometime before 1930 (likely closer to 1800), the star transitions from the compact, hot ($T_* \sim 40000$ K) state with a low density, high velocity wind to (on average) a cooler ($T_* \sim 7500$ K) star with a high density, lower velocity wind. Then, around 1955 (not 1960) the star undergoes an LBV (or other) eruption to produce the pre-peak luminosity plateau, accompanied by a further rise in the wind density and a higher wind velocity. The light curves in Branch & Greenstein (1971) and Doggett & Branch (1985) appear to allow the outburst phase to commence earlier than 1960 due to the poor quality of the magnitude limits from 1955 to 1960. Then in December 1961, the star undergoes core collapse and produces an SN, leading to the luminosity peak. The outgoing shock wave now interacts with the previous mass loss history, where the first, more luminous post-SN plateau is due to interactions with the LBV eruption ejecta, and the second, longer plateau is due to the wind emitted in the cool phase. The luminosity then drops dramatically when the shock wave reaches the low density wind of the pre-explosion hot star phase.

The observed velocities now represent the velocity of the expanding shock wave rather than the wind. Suppose we try to power the light curve using the luminosity available from shock heating the circumstellar medium (CSM),

$$L = \frac{v_s^3}{2v_w}\epsilon\dot{M} \simeq 10^{7.7}\left(\frac{\dot{M}}{10^{-2}M_\odot/\mathrm{year}}\right)\left(\frac{v_s}{4000\mathrm{km/s}}\right)^3\left(\frac{100\mathrm{km/s}}{v_w}\right)\left(\frac{\epsilon}{0.1}\right)L_\odot \tag{7}$$

where $\dot{M}$ is the mass loss rate, v_w is the wind velocity, v_s is the shock velocity and ϵ is the radiative efficiency (e.g. Chugai & Danziger 1994). Here we have scaled v_s to the 4000 km/s suggested by the VLBI observations of Chu et al. (2004). Using 2000 km/s simply drives the required mass loss rates upwards while making it easier to have extended, post-SN luminosity plateaus.

The difficult part about producing the first post-transient luminosity plateau is its duration. The length of the plateau t_p should be roughly $t_p \simeq t_e v_w/v_s$, where t_e is the duration of the eruption prior to 1961. If $t_e \simeq 1$ year and $t_p \simeq 0.5$ years, as in the description of the light curve by Goodrich et al. (1989), the required velocity ratio $v_w/v_s \simeq 1/2$ seems unphysical. However, if however, the eruption commenced closer to 1955, so that $t_e \simeq 5$ years, but was missed due to the shallowness of the observations (Branch & Greenstein 1971, Doggett & Branch 1985), then we need only have $v_s/v_s \simeq 1/10$. Suppose we adopt $v_s/v_w = 5$, then reproducing the plateau luminosity of order $L \simeq 2\times10^7 L_\odot$ ($m_{pg} \simeq 17$) requires a mass loss rate of

$$\dot{M} \simeq 0.03\left(\frac{4000\mathrm{km/s}}{v_s}\right)^2\left(\frac{5v_w}{v_s}\right)\left(\frac{0.1}{\epsilon}\right)M_\odot/\mathrm{year} \tag{8}$$

which is grossly consistent with an LBV eruption (Humphreys & Davidson 1994). This rises to $10^{-1}M_\odot$/year if we use $v_s = 2000$ km/s. In either case, enough mass is involved that we may be also be underestimating the radiative efficiency (see Smith & McCray 2007).

The shock then moves out through the lower density material from the earlier "S Doradus" phase – here we simply envision an extended period where the star is on average producing a relatively dense wind. The necessary shock luminosity is now 10 times lower, and we are free to make the ratio v_s/v_w much larger since we have no definitive time scale for the start of this phase beyond that it began before $\sim$ 1930. Thus, the mass loss rate need only be

$$\dot{M} \simeq 4\times10^{-4}\left(\frac{4000\mathrm{km/s}}{v_s}\right)^3\left(\frac{v_w}{100\mathrm{km/s}}\right)\left(\frac{0.1}{\epsilon}\right)M_\odot/\mathrm{year}, \tag{9}$$

which is relatively easy for an LBV produce even outside of eruptions. Here $v_s/v_w = 40$, so the enhanced mass loss phase would have started circa 1800 in order to make $t_p \simeq 4$ years. The biggest problem with this schematic is that the material ejected prior to the SN cannot itself form significant amounts of dust or the progenitor would have been self-obscured, similar to SN 2008S (see, e.g., Prieto et al. 2008).

Not only was the progenitor of SN 1961V massive, $M_{ZAMS} \gtrsim 80M_\odot$, but it must also have been relatively massive at death. While appearing to be rich in helium (Branch & Greenstein 1971), it was still a Type II SN, rather than a Type Ib or Ic. We found no detailed pre-supernova models for this mass and metallicity range, but it is in the regime that Heger et al. (2003) estimate would be weak Type Ib/c fall-back

SN leading to black hole formation. The solar metallicity models in Woosley et al. (2002) have already lost much of their helium to mass loss. For their low metallicity models (10^{-4} solar!), the star would need to be more massive at death than $M \simeq 30M_{\odot}$ in order to retain any hydrogen. If it was a fall-back SN forming a BH, SN 1961V was not notably sub-luminous. Alternatively, some massive stars may still form NSs, as suggested by the existence of a magnetar in Westerlund 1. The progenitor of this NS seems to require a $> 40M_{\odot}$ progenitor given the other massive stars in the cluster (Muno et al. 2006), unless it can be explained by binary evolution and mass transfer (Belczynski & Taam 2008). Since it takes virtually no mass to power accretion onto a $\sim 10M_{\odot}$ black hole at the Eddington limit compared to the ejected mass, we might expect the newly formed BH to accrete at the Eddington limit for an extended period of time. However, Perna et al. (2008) found no X-ray emission from the site to a limit of $L_X < 6 \times 10^{37}$ ergs/s (2-10 keV)[4] in March 2000, corresponding to a limit of order 5% of Eddington.

Finally, the existence of other Type IIn supernova requiring major mass loss events shortly before collapse changes our prior on the likelihood of such correlations for SN 1961V. Rather than being bizarre, it is simply the closest example, one which is so close that we could see the pre-SN activity. SN 1961V, SN 2005gl and their relatives are all cases where the correlated mass loss is large and dramatic. We usually assume that stars are evolving quasi-statically in their last phases, with no indicators of imminent death, yet this clearly does not hold for this class of objects. It is an interesting question whether this phenomenon is limited to a special class of SN, as proposed by Gal-Yam et al. (2007), or that we presently only notice the most dramatic examples of a more ubiquitous phenomenon. In either case, it appears that studies of SN progenitors should evolve from simple attempts to obtain a single snapshot of the star to monitoring their behavior over their final years.

We would like to thank John Beacom, José Prieto and Todd Thompson for discussions and comments, Rebecca Stoll for estimating the local gas phase metallicity, and Robert Soria and Rosalba Perna for providing a softer energy band X-ray flux limit. CSK, DMS and KZS are supported by NSF grant AST-0908816. This work is based in part on observations made with the Spitzer Space Telescope, which is operated by the Jet Propulsion Laboratory, California Institute of Technology under a contract with NASA, and in part on observations made with the NASA/ESA Hubble Space Telescope, obtained from the data archive at the Space Telescope Institute. STScI is operated by the association of Universities for Research in Astronomy, Inc. under the NASA contract NAS 5-26555. This research has made use of the NASA/IPAC Extragalactic Database (NED) which is operated by the Jet Propulsion Laboratory, California Institute of Technology, under contract with the National Aeronautics and Space Administration.

Facilities: Spitzer,HST

[4]With a similar limit of $< 2 \times 10^{37}$ ergs/s for the softer 0.3-8 keV band (Soria & Perna 2010, private communication).

REFERENCES

Alard, C., & Lupton, R. H. 1998, ApJ, 503, 325

Alard, C. 2000, A&AS, 144, 363

Belczynski, K., & Taam, R. E. 2008, ApJ, 685, 400

Bertola, F. 1963, Contributions dell'Osservatorio Astrofisica dell'Universita di Padova in Asiago, 142, 3

Bertola, F. 1964, Annales d'Astrophysique, 27, 319

Bertola, F. 1965, Contributions dell'Osservatorio Astrofisica dell'Universita di Padova in Asiago, 171, 3

Bertola, F. 1967, Information Bulletin on Variable Stars, 196, 1

Bertola, F., & Arp, H. 1970, PASP, 82, 894

Branch, D., & Greenstein, J. L. 1971, ApJ, 167, 89

Branch, D., & Cowan, J. J. 1985, ApJ, 297, L33

Ciatti, F., Rosino, L., & Bertola, F. 1971, Mem. Soc. Astron. Italiana, 42, 163

Chu, Y.-H., Gruendl, R. A., Stockdale, C. J., Rupen, M. P., Cowan, J. J., & Teare, S. W. 2004, AJ, 127, 2850

Chugai, N. N., & Danziger, I. J. 1994, MNRAS, 268, 173

Cowan, J. J., Henry, R. B. C., & Branch, D. 1988, ApJ, 329, 116

Crockett, R. M., et al. 2008, ApJ, 672, L99

Doggett, J. B., & Branch, D. 1985, AJ, 90, 2303

Table 1. Spitzer Observations of NGC 1058

date	MJD	PI/Program	3.6μm	4.5μm	5.8μm	8.0μm	24μm	70μm
2004-08-14	53231.31	Fazio/69	150	150	150	150	0	0
2004-08-25	53242.03	Fazio/69	0	0	0	0	10	9
2007-09-14	54357.66	Kotak/40619	300	300	300	300	0	0
2007-09-29	54372.22	Kotak/40619	0	0	0	0	30	0

Note. — Exposure times are in seconds. The IRAC frame times were 30 s in both observations.

Table 2. IRAC Photometry

Source	Aperture	[3.6] (mJy)	[4.5] (mJy)	[5.8] (mJy)	[8.0] (mJy)
SN1961V area	2.″4	0.0139 ± 0.0011	0.0104 ± 0.0014	0.0557 ± 0.0062	0.1682 ± 0.0096
	3.″6	0.0226 ± 0.0010	0.0160 ± 0.0019	0.0690 ± 0.0074	0.2070 ± 0.0108
SN1961V/#8	DAOPHOT	0.0078 ± 0.0010	0.0079 ± 0.0010	0.0288 ± 0.0098	0.0614 ± 0.0275
SN1961V/other	DAOPHOT	0.0084 ± 0.0008	0.0081 ± 0.0010	0.0096 ± 0.0041	0.0571 ± 0.0064
Star #3	2.″4	0.0071 ± 0.0013	0.0031 ± 0.0012	< 0.019	< 0.028
	3.″6	0.0044 ± 0.0021	0.0003 ± 0.0017	0.0102 ± 0.0084	0.0349 ± 0.0103
	DAOPHOT	0.0103 ± 0.0008	0.0073 ± 0.0010	...	...
Star A	2.″4	0.0190 ± 0.0010	0.0115 ± 0.0010	0.0346 ± 0.0070	0.0238 ± 0.0078
	3.″6	0.0204 ± 0.0017	0.0129 ± 0.0016	0.0566 ± 0.0075	0.0167 ± 0.0080
	DAOPHOT	0.0256 ± 0.0011	0.0151 ± 0.0013	...	...
Star B	2.″4	0.0147 ± 0.0018	0.0075 ± 0.0014	0.0209 ± 0.0092	0.0529 ± 0.0087
	3.″6	0.0196 ± 0.0029	0.0119 ± 0.0019	0.0605 ± 0.0081	0.0869 ± 0.0088
	DAOPHOT	0.0149 ± 0.0012	0.0094 ± 0.0011	...	...
Star C	2.″4	0.0064 ± 0.0012	0.0057 ± 0.0011	0.0367 ± 0.0051	0.1031 ± 0.0099
	3.″6	0.0073 ± 0.0019	0.0041 ± 0.0017	0.0251 ± 0.0063	0.1273 ± 0.0101
	DAOPHOT	0.0056 ± 0.0009	0.0062 ± 0.0012	...	...
SN 2007gr	2.″4	4.7079 ± 0.0207	3.7626 ± 0.0137	2.7023 ± 0.0431	2.4228 ± 0.1452
	3.″6	5.1208 ± 0.0313	4.0373 ± 0.0192	3.0947 ± 0.0225	3.4095 ± 0.1182
	DAOPHOT	5.6602 ± 0.1845	4.1676 ± 0.3363	...	...
SN 1969L	2.″4	0.0065 ± 0.0013	< 0.0060	0.0093 ± 0.0060	0.0165 ± 0.0101
	3.″6	0.0099 ± 0.0012	< 0.0065	0.0208 ± 0.0054	0.0013 ± 0.0047

Note. — Flux limits are 3σ limits.

Draine, B. T. 1981, ApJ, 245, 880

Draine, B. T., & Lee, H. M. 1984, ApJ, 285, 89

Eck, C. R., Cowan, J. J., & Branch, D. 2002, ApJ, 573, 306

Elitzur, M., & Ivezić, Ž. 2001, MNRAS, 327, 403

Fazio, G. G., et al. 2004, ApJS, 154, 10

Ferguson, A. M. N., Gallagher, J. S., & Wyse, R. F. G. 1998, AJ, 116, 673

Fesen, R. A. 1985, ApJ, 297, L29

Filippenko, A. V., Barth, A. J., Bower, G. C., Ho, L. C., Stringfellow, G. S., Goodrich, R. W., & Porter, A. C. 1995, AJ, 110, 2261

Filippenko, A. V. 1997, ARA&A, 35, 309

Gal-Yam, A., et al. 2007, ApJ, 656, 372

Gal-Yam, A., & Leonard, D. C. 2009, Nature, 458, 865

Goodrich, R. W., Stringfellow, G. S., Penrod, G. D., & Filippenko, A. V. 1989, ApJ, 342, 908

Heger, A., Fryer, C. L., Woosley, S. E., Langer, N., & Hartmann, D. H. 2003, ApJ, 591, 288

Humphreys, R. M., & Davidson, K. 1994, PASP, 106, 1025

Humphreys, R. M., Davidson, K., & Smith, N. 1999, PASP, 111, 1124

Ivezić, Ž., & Elitzur, M. 1997, MNRAS, 287, 799

Ivezić, Ž., Nenkova, M., & Elitzur, M. 1999, User Manual for DUSTY, University of Kentucky Internal Report http:www.pa.uky.edum̃oshedusty

Kewley, L. J., & Ellison, S. L. 2008, ApJ, 681, 1183

Khan, R., Stanek, K. Z., Prieto, J. L., Kochanek, C. S., Thompson, T. A., & Beacom, J. F. 2010, ApJ, 715, 1094

Klemola, A. R. 1986, PASP, 98, 464

Kochanek, C. S. 2009, ApJ, 707, 1578

Kozlowski, S., et al. 2010, arXiv:1006.4162

Li, W., Filippenko, A. V., Van Dyk, S. D., Hu, J., Qiu, Y., Modjaz, M., & Leonard, D. C. 2002, PASP, 114, 403

Marigo, P., Girardi, L., Bressan, A., Groenewegen, M. A. T., Silva, L., & Granato, G. L. 2008, A&A, 482, 883

Muno, M. P., et al. 2006, ApJ, 636, L41

Pastorello, A., et al. 2007, Nature, 447, 829

Pastorello, A., et al. 2010, arXiv:1006.0504

Perna, R., Soria, R., Pooley, D., & Stella, L. 2008, MNRAS, 384, 1638

Prieto, J. L., et al. 2008, ApJ, 681, L9

Prieto, J. L., Szczygiel, D. M., Kochanek, C. S., Stanek, K. Z., Thompson, T. A., Beacom, J. F., Garnavich, P. M., & Woodward, C. E. 2010, arXiv:1007.0011

Rieke, G. H., et al. 2004, ApJS, 154, 25

Schlegel, D. J., Finkbeiner, D. P., & Davis, M. 1998, ApJ, 500, 525

Schlegel, E. M. 1990, MNRAS, 244, 269

Semenov, D., Henning, T., Helling, C., Ilgner, M., & Sedlmayr, E. 2003, A&A, 410, 611

Smartt, S. J. 2009, ARA&A, 47, 63

Smith, N., & McCray, R. 2007, ApJ, 671, L17

Smith, N., Chornock, R., Li, W., Ganeshalingam, M., Silverman, J. M., Foley, R. J., Filippenko, A. V., & Barth, A. J. 2008, ApJ, 686, 467

Silbermann, N. A., et al. 1996, ApJ, 470, 1

Smith, N., Humphreys, R. M., & Gehrz, R. D. 2001, PASP, 113, 692

Smith, N., & Owocki, S. P. 2006, ApJ, 645, L45

Smith, N., et al., 2010, submitted to MNRAS

Stetson, P. B. 1987, PASP, 99, 191

Stockdale, C. J., Rupen, M. P., Cowan, J. J., Chu, Y.-H., & Jones, S. S. 2001, AJ, 122, 283

Utrobin, V. P. 1987, Soviet Astronomy Letters, 13, 50

Valenti, S., et al. 2008, ApJ, 673, L155

Van Dyk, S. D., Peng, C. Y., Barth, A. J., & Filippenko, A. V. 1999, AJ, 118, 2331

Van Dyk, S. D., Filippenko, A. V., & Li, W. 2002, PASP, 114, 700

Van Dyk, S. D., Filippenko, A. V., Chornock, R., Li, W., & Challis, P. M. 2005, PASP, 117, 553

Wagner, R. M., et al. 2004, PASP, 116, 326

Woosley, S. E., Heger, A., & Weaver, T. A. 2002, Reviews of Modern Physics, 74, 1015

Wright, E. L. 1980, ApJ, 242, L23

Zwicky, F. 1964, ApJ, 139, 514

This preprint was prepared with the AAS LaTeX macros v5.2.

Table 3. MIPS Photometry

Source	[24] (mJy)	[70] (mJy)
SN1961V area	0.226 ± 0.0039	< 8.0
Star #3	0.089 ± 0.0044	$\cdots$
Star A	0.043 ± 0.0082	$\cdots$
Star B	0.094 ± 0.0080	< 190
Star C	0.027 ± 0.0049	< 178
SN 2007gr	3.155 ± 0.0398	$\cdots$
SN 1969L	< 0.063	$\cdots$

Note. — Flux limits are 3σ limits.